UNIVERSITY OF BIRMINGHAM
University of Birmingham Research at Birmingham

Additive manufactured millimeter wave off-axis bull's-eye antenna

Beaskoetxea, Unai; Maci, Stefano; Navarro-Cia, Miguel; Beruete, Miguel

DOI:
10.23919/EuCAP.2017.7928480

License:
None: All rights reserved

Document Version
Peer reviewed version

Citation for published version (Harvard):
Beaskoetxea, U, Maci, S, Navarro-Cia, M & Beruete, M 2017, Additive manufactured millimeter wave off-axis bull's-eye antenna. in *2017 11th European Conference on Antennas and Propagation, EUCAP 2017.*, 7928480, Institute of Electrical and Electronics Engineers (IEEE), pp. 2503-2506, 11th European Conference on Antennas and Propagation, EUCAP 2017, Paris, France, 19/03/17. https://doi.org/10.23919/EuCAP.2017.7928480

Link to publication on Research at Birmingham portal

Publisher Rights Statement:
Eligibility for repository: Checked on 27/6/2017

General rights
Unless a licence is specified above, all rights (including copyright and moral rights) in this document are retained by the authors and/or the copyright holders. The express permission of the copyright holder must be obtained for any use of this material other than for purposes permitted by law.

•Users may freely distribute the URL that is used to identify this publication.
•Users may download and/or print one copy of the publication from the University of Birmingham research portal for the purpose of private study or non-commercial research.
•User may use extracts from the document in line with the concept of 'fair dealing' under the Copyright, Designs and Patents Act 1988 (?)
•Users may not further distribute the material nor use it for the purposes of commercial gain.

Where a licence is displayed above, please note the terms and conditions of the licence govern your use of this document.

When citing, please reference the published version.

Take down policy
While the University of Birmingham exercises care and attention in making items available there are rare occasions when an item has been uploaded in error or has been deemed to be commercially or otherwise sensitive.

If you believe that this is the case for this document, please contact UBIRA@lists.bham.ac.uk providing details and we will remove access to the work immediately and investigate.

Download date: 26. Apr. 2024

Additive Manufactured Millimeter Wave Off-Axis Bull's-Eye Antenna

Unai Beaskoetxea[(1)], Stefano Maci [(2)], Miguel Navarro-Cía [(3)] and Miguel Beruete [(1,4)]
unai.beaskoetxea@unavarra.es, macis@dii.unisi.it, m.navarro-cia@bham.ac.uk, miguel.beruete@unavarra.es
[(1)] Dpto. Ingeniería Eléctrica y Electrónica, Universidad Pública de Navarra, Spain
[(2)] Department of Information Engineering, University of Siena, Italy
[(3)] School of Physics and Astronomy, University of Birmingham, United Kingdom
[(4)] Institute of Smart Cities, Universidad Pública de Navarra, Spain

***Abstract*- Despite their low profile and competitive radiation characteristics, most of the devices in the corrugated leaky wave antenna family feature an unnecessary excess weight which result detrimental for current innovative applications, such as unmanned aerial vehicles (UAV), aircrafts or satellite antennas. Stereolitography, accompanied by plating, is presented as an economic and fast solution for the manufacturing of lightweight devices, which at the same time is able to overcome traditional metal drilling/spark erosion manufacturing limitations, like the impossibility of eroding extremely narrow grooves. Here we present an elliptical Bull's-Eye antenna operating at 96 GHz fabricated following a 3D-printing and copper coating process. Due to its off-centered grooves distribution, a tilted beam pointing at 16.5º is obtained, presenting a gain of 17 dB and 3.5 beamwidth. The theoretical analysis conducted to obtain the equations which govern the grooves distribution and shape is also presented. This prototype results of interest for point-to-point communications where direct front side view is not possible, as well as for applications where lightweight and cost-effective antennas are needed, such as satellite communications or deployed in UAV's.**

I. Introduction

The radiation efficiency and reduced volume of leaky wave antennas [1]–[6] is nowadays well known and, indeed, they are quite interesting for applications where this low profile is a prerequisite. Nevertheless, most of the metal-based structures antennas [7]–[10] present a weight which might be a handicap for applications where light-weight is an issue is directly linked to the cost, as satellite or drones deployment. 3D printing is already proving useful in several everyday areas like prosthesis, in the automotive sector or even in the toy industry. Thus, it is easy to understand an equivalent importance in the manufacturing of complex geometries antennas.

In this work, we present a copper coated 3D printed antenna that weighs including screws less than a fourth of a solid copper antenna. It was designed such that a high gain beam pointing at 16.5º, rather than at broadside [11], is obtained. The distribution and shape of the employed elliptical grooves is backed up by a theoretical analysis of the physical mechanism of the leaky wave propagation. The experimental results (peak gain of 17 dB with a narrow beamwidth of approximately 3.5º) resemble the simulations; the observed quantitative disagreement comes from ignoring the fabrication tolerances in the model, as refined simulations confirm. A more comprehensive work can be found in [12].

II. Theoretical Analysis of Groove Design and Distribution

A 3D view of the scheme used for the theoretical analysis of the off-axis beaming antenna is shown in Fig. 1(a). The observed asymmetry in both half-planes in the *y* direction (defining the half-part of the antenna with $y > 0$ as *forward* and the half part with $y < 0$ as *backward*, Fig. 1(b)) allows tilted beaming in a direction governed by the interaction between the cylindrical wavefront of the wave launched by the central open ended waveguide and the elliptical grooves. The antenna is designed in such a way that the forward part, supporting a forward leaky-mode, and the backward part, supporting a backward leaky-mode, generate a beam in the same direction θ at a certain frequency, Fig. 1(a).

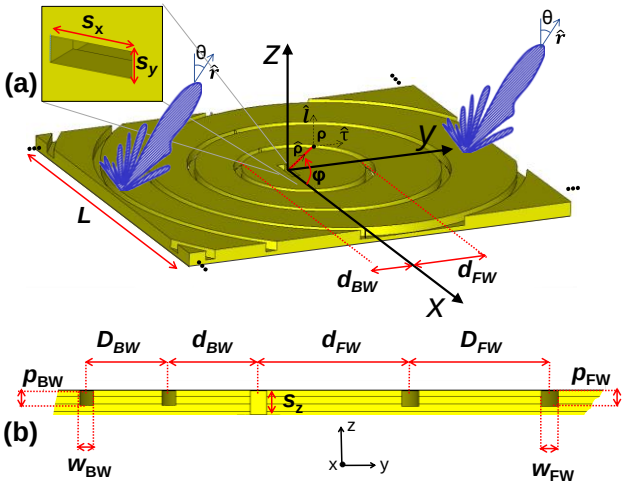

Fig.1 Geometry of analyzed structure. (a) 3D view. (b) Cross-sectional view in the plane z-y.

Let us take the radiating aperture as the center of our cylindrical coordinate system, with ρ, φ the coordinates of the observation point on the surface of the structure. The central aperture excites a grazing wave propagating with electric field normal to the surface and cylindrical wavefront which interacts with the grooves that produce the leakage at an angle controlled by the groove period. The axis of the first groove is given by the polar coordinate equation $\rho = d(\varphi)$, where $\varphi \in (0º, 180º)$ for the *forward* part and $\varphi \in (180º, 360º)$ for the *backward* part. The analytical expression of this polar coordinate equation, for which a phase-coherence condition

for the scattered field from the first curvilinear groove in a direction $\hat{r}' = \cos\theta'\,\hat{z} + \sin\theta'\,\hat{y}$ is ensured, can be formulated as:

$$kd(\varphi) + k\left[r - d(\varphi)\hat{\rho}\cdot\hat{r}'\right] = kd_0 + kr \quad , \quad \varphi \in (0,2\pi) \quad (1)$$

with r the far field distance from the origin, $\hat{\rho} = \cos\varphi\hat{x} + \sin\varphi\hat{y}$ the ray direction, k the free-space radial wavenumber and $d_0 = d(\varphi = 0)$ the distance in the x direction to the first groove. Since $\hat{\rho}\cdot\hat{r}' = \sin\theta'\sin\varphi$, we may rewrite (1) as:

$$d(\varphi) = \frac{d_0}{1 - \sin\theta'\sin\varphi} \;\; ; \;\; \varphi \in (0,2\pi) \qquad (2)$$

which defines the equation of the first groove as an ellipse with a focus at the origin. The intersection distances of the first annular groove with the y axis (d_{FW} and d_{BW}) are obtained by substituting $\varphi = \pi/2$ and $\varphi = 3\pi/2$ in (2). The equations of the remaining grooves are found by replacing kd_0 with $kd_0 + 2n\pi,\ n = 0,1,2,..,$ at the right hand side of (1):

$$d^{(n)}(\varphi) = \frac{d_0 + n\lambda}{1 - \sin\theta'\sin\varphi} \;\; , \; n = 0,1,2,..P \qquad (3)$$

with λ the operation frequency (free space wavelength) and n the index of the P periods. This implies that all rings radiate in phase with the first (n = 0) ring. Given that sinφ is positive the interspace between grooves in the forward region ($D(\varphi) = \lambda/(1 - \sin\theta'\sin\varphi)$) is larger than the wavelength. In contrast, the groove spacing is less than a wavelength in the backward region, as sinφ is negative. The space in the y direction between two consecutive grooves is, for the forward and backward regions respectively:

$$D_{FW} = \lambda/(1 - \sin\theta'); \quad D_{BW} = \lambda/(1 + \sin\theta') \qquad (4)$$

The arbitrary constant d_0 and the interspace distances, must go through an optimization routine (based on the Trust Region Framework), setting as a goal to achieve the highest possible gain at θ = 15° and as lowest side lobe level as possible at the design frequency. In order to excite the TE_{11} mode (i.e., fundamental mode of the coaxial waveguide formed by each groove), grooves must present a depth $p < \lambda/4$ and a width $w << \lambda$ (as observed in previous works) and, due to the asymmetry of the structure with respect to the x axis, both parameters have to be simultaneously optimized in the forward and backward parts.

III. Prototype Design and Simulation Results

The antenna was designed and studied using the commercial simulator CST Microwave Studio™ [13]. Its response was simulated form 85 GHz to 105 GHz, with a step of 100 MHz step. A magnetic symmetry was defined in the y-z plane and a non-uniform hexahedral mesh with smallest mesh cell of 44 μm × 32 μm × 127 μm (13.66λ × 9.93λ × 39.4λ) was used to map accurately the geometry. The metallization of the antenna was modelled as bulk Copper ($\sigma = 5.8\times10^7$ S/m). The antenna follows a design process similar to previous antennas [7], [8] where a metallic slab is perforated by a central aperture, whose dimensions ($s_x \times s_y \times s_z$) fix the frequency at which the power, fed by a waveguide attached to the rear part, will be coupled to a TM surface wave. In this case, the slot's width (1.627 mm) and the height (0.470 mm) fix the operating transversal resonance and its Q-factor, whereas the slot's depth (0.77 mm) locates the longitudinal resonance at higher frequencies. As the slot's depth corresponds to the thickness of the metal slab, it is possible to obtain a structure as thin as the corrugations depth allow. For an antenna working at 96 GHz it is necessary to use a standard WR-10 waveguide (W-Band, 75-110 GHz). Once the whole antenna was designed, the optimization routine returned d_0 = 3.189 mm, D_{FW} = 4.142 mm and D_{BW} = 2.438 mm, whereas the grooves presented final width and depth values between 420 mm and 520 mm.

Red curves in Fig. 2 correspond to the simulation results. The S_{11} (Fig. 2(a)) presents a dip at f = 93 GHz, approximately $\lambda/2$ (s_x/2), frequency at which the maximum realized gain (20.35 dB) is obtained (Fig. 2(b)). In the range from ~90 GHz to 97 GHz the radiated beam points at ~15º (Fig. 2(c)), while the realized gain is over 15 dB, the beamwidth is approximately 6º ((Fig. 2(d)) and the return loss is below -10 dB. This reveals that the proposed structure presents in this bandwidth a good frequency-stable radiation behavior. Evidently, the narrowest beam (5.1º) and a precise pointing at 15º is obtained at f = 93 GHz, the frequency of design. It was chosen to include only P = 7 rings, as it was found to be a good tradeoff between size and gain. A higher gain is not necessarily obtained with an increasing number of periods, as reported in [7], [8], [14].

IV. Fabrication And Experimental Results

3D printing allows fast prototyping light antennas at a competitive price compared to traditional milling machining. Nevertheless, as the metallization of the inner surface of the slot and waveguide would present an increased difficulty, it was decided to print the antenna in two splitted blocks (splitted along the electric (y-z) plane, which also minimizes spurious radiation losses [15]), thus facilitating the metallization process. Both blocks were manufactured by means of a Stereolitography (SLA) additive process, where successive photo reactive liquid resin layers are cured by an ultra-violet light beam, resulting in solid stacked layers. Then, it was carried out the metallization process, consisting of a four stage chemical process, to imbue both pieces with conductivity, and an electro-less nickel layering followed by a 30 μm thick copper layer electro-plating-process-based deposition. The nickel layer is necessary to improve the adhesion of the copper to the structure. Finally the metallized halves were fastened by means of light screws (with an overall weight of 50.95 g). The total weight of the final structure (Fig. 3), including the fasteners, was 111.2 g, far from the equivalent weight of a solid copper antenna, which would weight ~ 456 g (with copper's density = 8.9 g/cm^3). Hence, a 75% lighter antenna, considering the fasteners, was obtained.

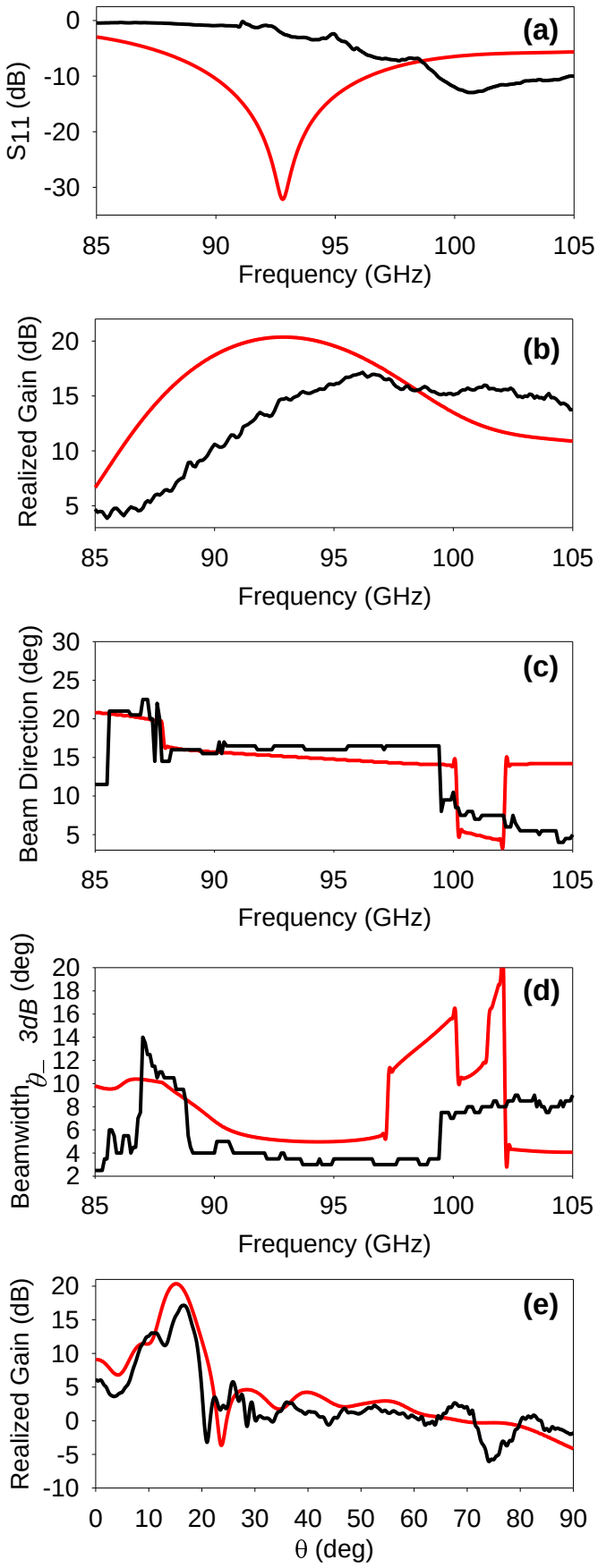

Fig. 2 Simulation (red curves) and experimental (black curves) results. (a) S11. (b) Realized gain. (c) Beam Direction. (d) Beamwidth. (e) E-plane radiation diagram at the frequency of the maximum gain (f = 93 GHz for simulation, f = 96 GHz for measurement).

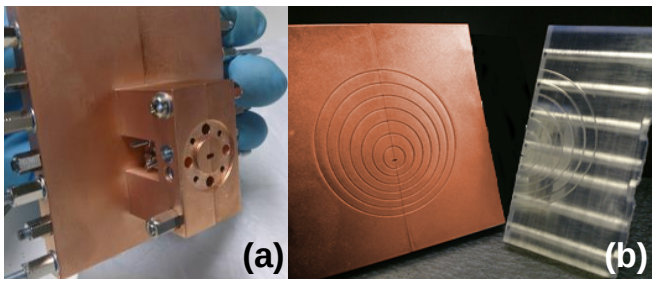

Fig. 3 Manufactured antenna. (a) Back view. (b) Front view of one half of the uncoated prototype and of the final structure.

The scrutiny of the antenna's dimensions by means of an electronic microscope revealed certain inaccuracies in the fabrication process, such as a 123 µm narrower slot width and up to 160 µm narrower grooves in both forward and backward regions (350 µm and 260 µm, respectively). These deviations from the ideal design led to different radiation characteristics.

In order to obtain the radiation characteristics of the antenna, it was used an ABmm^{TM} Quasioptical Vector Network Analyzer. The E-plane radiation was acquired facing the BE antenna (mounted over an azimuth-rotary platform) and a standard W-band corrugated horn antenna at a distance of 4.5 m, 1.10 m above the floor. All surfaces susceptible of producing reflections were covered with radar absorbing material. The broadband gain, recorded from 0 to 90º, with a step of 0.5º, and from 85 to 105 GHz with a step of 100 MHz, was obtained by applying the gain comparison method [16].

While the simulated return loss presents a dip at 92.8 GHz (frequency of design), the experimental result (black curve in Fig. 2 (a)) shows a red-shift of the dip frequency towards higher values. Furthermore, when compared to the simulation result, a decrease of 3 dB of the maximum gain (17 dB) and a 4 GHz shifting of its location towards higher frequencies is observed (black curve in Fig. 2(b)). This might be due to the aforementioned fabrication tolerances. Black curves in Fig. 2 (c) and (e) display the beam direction and the E-plane radiation diagram, respectively. It can be seen that, although the experimental beam direction remains stable with frequency (as the simulated one did), it now points at approximately 16.5º in the band of interest. The decrease of the experimental gain peak and its shifting towards 16.5º is easily observed in the E-plane radiation diagram when compared with the simulated diagram. Nevertheless, a narrower beam is also observed for almost all the band under consideration, obtaining a minimum value of θ_{-3dB} = 3.5º at the frequency of the maximum experimental gain (Fig. 2(d)). It is also interesting to address the trend of the beamwidth values from 98 GHz to 103.5 GHz. At f = 98 GHz, the single beam splits in two beams, corresponding to the forward and backward parts contributions. As frequency is swept towards higher frequencies, the separation between beams is increased, but still appear as a single increasingly wider beam. From f ~102 GHz to f ~103.5 GHz, both beams appear clearly separated, presenting the backward contribution the largest amplitude, thus fixing the beam direction (Fig. 2(d)) to ~3.5º. As the backward beam melts with a contiguous lobe, it can be observed a wide θ_{-3dB} = 25º beam at f ~ 103.5 GHz. Then, its amplitude decreases, becoming the forward beam

the dominant one, thus fixing the beam direction at ~14º and presenting θ_{-3dB} = 4.8º. The apparent inconsistency of having a measured narrower beam along a lower gain can be explained by the fact of the alteration of the optimum design, which results in a less efficient merging of both narrow forward and backward beams.

This deviation from the ideal case can be related with the previously mentioned fabrication tolerances, as well as with extra-losses due to metal roughness and experimental errors. Thus, for example, the red-shifting of the maximum gain peak might be due to the excitation of the TE_{11} mode at a higher frequency as a result of the narrower grooves. However, despite this, both structures show an overall good agreement and the manufactured prototype is shown to be an interesting solution to replace full metal antennas.

V. Conclusions

In this work we have presented a cost-effective metal-coated 3D printed antenna with good radiation characteristics. The structure, fabricated by means of SLA and then copper-plated by means of several chemical and plating steps process, due to its off-center distributed elliptical grooves, displays a beam pointing at 16.5º (interesting for point-to-point communications where tilted beaming is required). The equations that govern the corrugations shape and distribution as well as the analysis of the leaky wave carried out to obtain the final formulation have also been presented. The fabricated antenna displays a 17 dB beam with θ_{-3dB} = 3.5º at f = 96 GHz, thus showing an overall good agreement with the numerical results (when fabrication tolerances and experimental inaccuracies are taken into account) and a 75% lighter weight. It has been shown that, thanks to 3D printing and metal-coating, it is feasible to obtain, in a fast and cheap way, antennas which are a good solution to replace fully metal structures (heavy for some applications such as drones, UAV's or satellites, where excess weight is avoided).

Acknowledgment

This work was supported by the Spanish Government under contract TEC2014-51902-C2-2-R. U.B is financed under a grant from the Public University of Navarre. M. N.-C. is supported by University of Birmingham [Birmingham Fellowship]. M.B. acknowledges support by the Spanish Government under contract RYC-2011-08221.

References

[1] W. W. Hansen, "Radiating Electromagnetic Waveguide," U.S. Patent 2402622, 1946.

[2] R. A. Sigelmann and A. Ishimaru, "Radiation from periodic structures excited by an aperiodic source," *IEEE Trans. Antennas Propag.*, vol. 13, pp. 354–364, 1965.

[3] A. A. Oliner and D. R. Jackson, "Leaky-Wave Antennas," in *Antenna Engineering Handbook*, Mc Graw-Hi., J. L. Volakis, Ed. New York: Mc Graw-Hill, 2007, pp. 11–1/11–56.

[4] D. R. Jackson, C. Caloz, and T. Itoh, "Leaky-Wave Antennas," *Proc. IEEE*, vol. 100, no. 7, pp. 2194–2206, Jul. 2012.

[5] S. K. Podilchak, P. Baccarelli, P. Burghignoli, A. P. Freundorfer, and Y. M. M. Antar, "Analysis and Design of Annular Microstrip-Based Planar Periodic Leaky-Wave Antennas," *IEEE Trans. Antennas Propag.*, vol. 62, no. 6, pp. 2978–2991, 2014.

[6] F. Monticone and A. Alù, "Leaky-Wave Theory, Techniques, and Applications: From Microwaves to Visible Frequencies," *Proc. IEEE*, vol. 103, no. 5, pp. 793–821, 2015.

[7] M. Beruete, I. Campillo, J. S. Dolado, J. E. Rodríguez-Seco, E. Perea, F. Falcone, and M. Sorolla, "Very Low-Profile 'Bull's Eye' Feeder Antenna," *IEEE Antennas Wirel. Propag. Lett.*, vol. 4, no. 2, pp. 365–368, 2005.

[8] U. Beaskoetxea, V. Pacheco-Peña, B. Orazbayev, T. Akalin, S. Maci, M. Navarro-Cía, and M. Beruete, "77 GHz High Gain Bull's-Eye Antenna With Sinusoidal Profile," *IEEE Antennas Wirel. Propag. Lett.*, vol. 14, pp. 205–208, 2015.

[9] C. J. Vourch and T. D. Drysdale, "V-Band 'Bull's Eye' Antenna for CubeSat Applications," *IEEE Antennas Wirel. Propag. Lett.*, vol. 13, pp. 1092–1095, 2014.

[10] C. J. Vourch and T. D. Drysdale, "V-band Bull's eye antenna for multiple discretely steerable beams," *IET Microwaves, Antennas Propag.*, vol. 10, no. 3, pp. 318–325, 2016.

[11] M. Guglielmi and D. R. Jackson, "Broadside Radiation from Periodic Leaky- Wave Antennas," *IEEE Trans. Antennas Propag.*, vol. 41, no. 1, pp. 31–37, 1993.

[12] U. Beaskoetxea, S. Maci, M. Navarro-Cía, and M. Beruete, "3D-Printed 96 GHz Bull's-Eye Antenna with Off-Axis Beaming," *IEEE Trans. Antennas Propag.*, no. Submitted for Publication.

[13] www.cst.com, "CST Microwave Studio." .

[14] M. Beruete, I. Campillo, J. S. Dolado, E. Perea, F. Falcone, and M. Sorolla, "Dual-band low-profile corrugated feeder antenna," *IEEE Trans. Antennas Propag.*, vol. 54, no. 2, pp. 340–350, 2006.

[15] M. D. Auria, W. J. Otter, J. Hazell, B. T. W. Gillatt, C. Long-collins, and N. M. Ridler, "3-D Printed Metal-Pipe Rectangular Waveguides," *IEEE Trans. Components, Packag. Manuf. Technol.*, vol. 5, no. 9, pp. 1339–1349, 2015.

[16] "IEEE Standard Test Procedures for Antennas," *ANSI/IEEE Stand. 149-1979*, 1979.